

## Research



**Cite this article:** Michaels TCT, Mahadevan L.

2023 Optimal intercellular competition in senescence and cancer. *Proc. R. Soc. A* **479**: 20230204.

<https://doi.org/10.1098/rspa.2023.0204>

Received: 26 March 2023

Accepted: 4 August 2023

**Subject Areas:**

applied mathematics, statistical physics, complexity

**Keywords:**

multicellularity, cooperation and competition, senescence, cancer, ageing

**Authors for correspondence:**

Thomas C. T. Michaels

e-mail: [thomas.michaels@bc.biol.ethz.ch](mailto:thomas.michaels@bc.biol.ethz.ch)

L. Mahadevan

e-mail: [lmahadev@g.harvard.edu](mailto:lmahadev@g.harvard.edu)

# Optimal intercellular competition in senescence and cancer

Thomas C. T. Michaels<sup>1,2</sup> and L. Mahadevan<sup>3</sup>

<sup>1</sup>Department of Biology, Institute of Biochemistry, ETH Zurich, Otto Stern Weg 3, 8093 Zurich, Switzerland

<sup>2</sup>Bringing Materials to Life Initiative, ETH Zurich, Switzerland

<sup>3</sup>School of Engineering and Applied Sciences, Departments of Physics and Organismic and Evolutionary Biology, Harvard University, Cambridge, MA 02138, USA

LM, 0000-0002-5114-0519

Effective multicellularity requires both cooperation and competition between constituent cells. Cooperation involves sacrificing individual fitness in favour of that of the community, but excessive cooperation makes the community susceptible to senescence and ageing. Competition eliminates unfit senescent cells via natural selection and thus slows down ageing, but excessive competition makes the community susceptible to cheaters, as exemplified by cancer and cancer-like phenomena. These observations suggest that an optimal level of intercellular competition in a multicellular organism maximizes organismal vitality by delaying the inevitability of ageing. We quantify this idea using a statistical mechanical framework that leads to a generalized replicator dynamical system for the population of cells that changes their vitality and cooperation due to somatic mutations that make them susceptible to ageing and/or cancer. By accounting for the cost of cooperation and strength of competition in a minimal setting, we show that our model predicts an optimal value of competition that maximizes vitality and delays the inevitability of senescence or cancer. The results have implications for the design of strategies aimed at delaying ageing in biological, technical and social systems that exhibit similar processes.

## 1. Introduction

The evolution of multicellularity is linked to the advantages of collective physiology and behaviour absent in unicellular life, which include, but are not limited to [1–4]: division of labour, adaptation to varied environments, efficient use of resources, creation and maintenance of extracellular environmental niches, the collective inhibition of cell proliferation and programmed cell death. All these benefits of multicellular life require cooperation—the coordinated orchestration of functions that are essential for the development and maintenance of a complex organism. Cooperation, however, comes with a cost to individual cells that need to invest a part of their resources into traits that contribute positively to organismal vitality but reduce individual cell fitness [5–7].

Cooperation in multicellular organisms creates interdependence among cells, which in turn leads to damage accumulation, gradual decay and ageing. Indeed, it has been shown that many complex systems with multiple connected components (including both biologically evolved organisms and artificially engineered systems) in general experience ageing as a result of the interdependence between the components [8–13]. To ameliorate the consequences of degradation induced by ageing in both evolved and engineered systems requires continuous maintenance and repair. In multicellular organisms, a particular form of maintenance, controlled cell proliferation, increases the risk of accumulating deleterious heritable somatic mutations that cause the progressive decline of cellular function and, eventually, an irreversible arrest of cell growth, i.e. cellular senescence [14–16]. The accumulation of senescent cells results in a progressive loss of organismal vitality and a number of ageing-related pathologies [16,17].

In multicellular organisms with renewable tissues, senescent cells can be eliminated through natural selection as a result of the reduced fitness of senescent cells compared with healthy cells [5,16–20]. The resulting intercellular competition serves to increase organismic vitality at a cost associated with proliferation-driven renewal. The potential for the breakdown of cellular cooperation driven by excessive proliferation can lead to inappropriate cell survival, resource monopolization, abnormal cell differentiation, or degradation of the extracellular environment, which are considered hallmarks of cancer [2,21–24]. This is a form of cheating that emerges in a competitive environment because uncooperative cancerous cells enjoy a higher fitness relative to cooperative healthy cells and have an advantage in selection [5]. Then individually uncooperative cells can thrive (transiently) in a competitive environment, with deleterious consequences for the (long-term) collective vitality of the organism [25].

Thus intercellular competition in multicellular organisms is a double-edged sword: without competition, multicellularity is susceptible to senescence, while too much competition can lead to cheating and cancer or cancer-like phenomena [2,23]. Recently, an elegant study [14] builds on this idea suggesting that senescence and cancer are an inevitable consequence of the dilemma posed by competition that cannot be too weak or too strong, and spawned a series of commentaries on the generality of the conclusions [26–28]. Some questions that naturally arise in this context include the possibility of a minimal analytic framework that might help to uncover the essence of the arguments, while also posing the problem of whether there is an optimal level of competition that maximizes organismal vitality by controlling or delaying senescence without succumbing to cancer?

Here, we attempt to answer this question in terms of an approach based on a probabilistic master equation. We show that this leads to an analytically tractable mathematical model for the dynamics of multicellular ageing in terms of a modified form of generalized replicator dynamics. Our solvable model reveals the fundamental factors controlling the optimal level of intercellular competition in terms of two parameters that characterize the base fitness and vitality in the system. Our solution reveals the fundamental biophysical factors controlling the level of intercellular competition and predict an optimal value of this parameter that maximizes system vitality by delaying the inevitability of senescence or cancer. By providing a minimal statistical mechanical framework for the study of the collective vitality of a system, our results may motivate

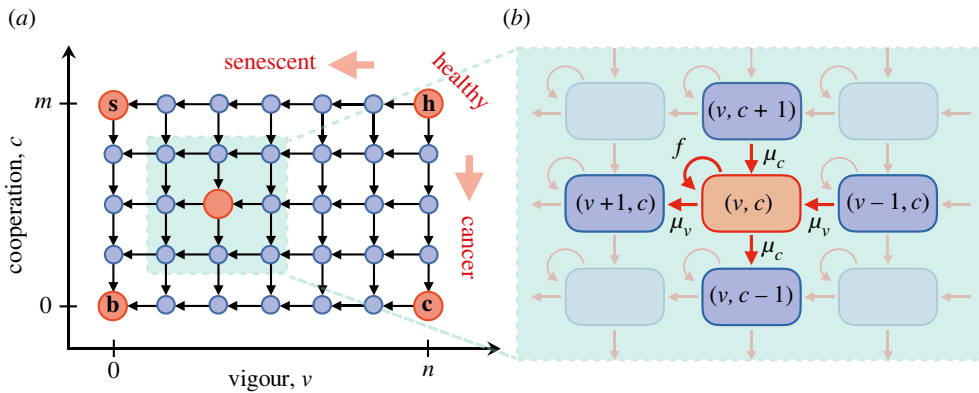


**Figure 1.** Master equation for multicellular ageing. (a) Cell vigour  $v$  and cooperation  $c$  define a two-dimensional coordinate system  $(v, c)$  of cell types. Progressive loss of vigour corresponds to cell senescence, while progressive loss of cooperation corresponds to cancer. The dynamics of the population  $N(v, c, t)$  of cells of type  $(v, c)$  at time  $t$  are described in terms of transition rates between different states  $(v, c) \rightarrow (v', c')$ . (b) The inset illustrates the different fluxes away from and into state  $(v, c)$ : (i) each cell type  $(v, c)$  proliferates with state-dependent rate  $f(v, c)$ ; (ii) mutations correspond to transitions that lower vigour ( $v \rightarrow v - 1$ , with rate  $\mu_v$ ) or cooperation ( $c \rightarrow c - 1$ , with rate  $\mu_c$ ).

the rational design of strategies for delaying ageing in biological, technical or social systems, where processes similar to those considered here are at play.

## 2. Dynamics of multicellular ageing

To describe the dynamics of multicellular ageing, we use a master equation approach in the space of cell types, as an equivalent to the Price equation formalism [29–31] (see appendix A for a master equation formulation of the Price equation). Following a previous study [14], we classify cell types in terms of two traits: vigour  $v$  and cooperation  $c$ . Vigour  $v$  is used as a general measure of cellular resources or function, e.g. metabolic activity. Cooperation  $c$  describes the fraction of resources that a cell devotes in activities that favour the functioning of the multicellular organism, including controlling homeostasis or maintaining the extracellular infrastructure. Since it is measured in terms of the fraction of the vigour, we expect it to be an intensive variable. Vigour and cooperation define a coordinate system of discrete cell types  $(v, c)$ ; in the simplest setting, we assume that  $v$  and  $c$  take discrete values in the range  $0 \leq v \leq n$  and  $0 \leq c \leq m$  (figure 1a) (a formulation using continuous values of these variables does not lead to results that are qualitatively different—see appendix C). Cells with high vigour ( $v = m$ ) and high cooperation ( $c = m$ ) are ‘healthy’ ( $h$ ), cell types that have lost vigour ( $v = 0$ ) are ‘senescent’ ( $s$ ), while cells with  $c = 0$  are ‘cancerous’ ( $c$ ) [14]. A fraction of cancer cells can undergo senescent transformations, leading to a group of cells in state  $(v = 0, c = 0)$  that are both senescent and cancerous ( $b$ ) [32]. Cells with intermediate values of  $v$  and  $c$  represent types that are not fully degraded; this situation mimics the fact that multiple mutations are necessary to induce senescence or cancer [33].

### (a) Cell populations

To quantify the time evolution of the (average) population  $N(v, c, t)$  of cells in state  $(v, c)$  at time  $t$ , we use a (mean field) master equation approach [34]. This captures spontaneous transitions between states in the coordinate system  $(v, c)$ . In our system, transitions occur as a result of two effects (figure 1): (i) cell proliferation (i.e. intercellular competition) at a rate  $f(v, c)$  and (ii) somatic mutations, which are permanent changes of cell genotype that lead to a gradual decline of vigour or cooperation phenotypes. In the following, we shall use the terms fitness and competition

interchangeably to denote the proliferation rate  $f(v, c)$ . We consider somatic mutations that affect only one of the two traits  $v$  or  $c$  in single steps with (state-dependent) rates  $\mu_v v$ , respectively,  $\mu_c c$  [14], but note that our framework can in principle be generalized to account for more complex transitions. Then the master equation describing the time evolution of  $N(v, c, t)$  is given by

$$\begin{aligned} \frac{\partial N(v, c, t)}{\partial t} = & f(v, c) N(v, c, t) \\ & + \mu_v (v + 1) N(v + 1, c, t) - \mu_v v N(v, c, t) \\ & + \mu_c (c + 1) N(v, c + 1, t) - \mu_c c N(v, c, t). \end{aligned} \quad (2.1)$$

The first term on the right-hand side of equation (2.1) describes the proliferation of  $N(v, c, t)$  with growth rate  $f(v, c)$ . The remaining terms in equation (2.1) describe the effect of somatic mutations by means of reaction fluxes away from and into the different cell types, i.e.  $N(v, c, t)$  decreases due to transitions  $v \rightarrow v - 1$  and  $c \rightarrow c - 1$ ; conversely,  $N(v, c, t)$  increases through transitions  $v + 1 \rightarrow v$  or  $c + 1 \rightarrow c$ .

## (b) Cell fractions

Since it is more useful to consider the dynamics of population fractions rather than the time evolution of various cell populations, we define the fraction of cells in state  $(v, c)$  at time  $t$  as

$$\rho(v, c, t) = \frac{N(v, c, t)}{N(t)} \quad \text{and} \quad N(t) = \sum_{v, c} N(v, c, t), \quad (2.2)$$

where  $N(t)$  is the total population of cells. We can then use equation (2.1) and derive a dynamic equation for  $\rho(v, c, t)$  (see appendix A) as

$$\begin{aligned} \frac{\partial \rho(v, c, t)}{\partial t} = & (f(v, c) - \bar{f}(t)) \rho(v, c, t) \\ & + \mu_v (v + 1) \rho(v + 1, c, t) - \mu_v v \rho(v, c, t) \\ & + \mu_c (c + 1) \rho(v, c + 1, t) - \mu_c c \rho(v, c, t), \end{aligned} \quad (2.3a)$$

where

$$\bar{f}(t) = \sum_{v, c} f(v, c) \rho(v, c, t), \quad (2.3b)$$

is the (time-dependent) average competition. Compared with equation (2.1), the key difference of equation (2.3a) lies in the first line, which describes the effect of selection: cell types with  $f > \bar{f}$  will be enriched by selection (fitness is higher than average), while those with  $f < \bar{f}$  will decrease in frequency over time (fitness lower than average). Equation (2.3a) is thus an extension of the replicator equation [35] that accounts for mutation fluxes changing cell type. Note that while the master equation for cell populations (2.1) is linear, the equation for cell fractions (2.3a) is nonlinear. Also note that the master equation is a deterministic equation describing the average population or fraction of cells of a certain type, while  $v$  and  $c$  are stochastic variables, capturing stochasticity in the appearance of mutations or in cell proliferation. Alternative methods commonly used in population genetics include PDE-based approaches such as the Fokker–Planck formalism [36], which follow from the master equation through Taylor-series expansion in  $v$  and  $c$ ; here we stay with the ME approach for generality.

We choose the mutation rates  $\mu_v$ ,  $\mu_c$  to be linearly dependent on  $v$  and  $c$  respectively for simplicity. This choice guarantees that in the absence of selection the average vigour  $\bar{v}(t) = \sum_{v, c} v \rho(v, c, t) \propto e^{-\mu_v t}$  and cooperation  $\bar{c}(t) = \sum_{v, c} c \rho(v, c, t) \propto e^{-\mu_c t}$  decay exponentially with rates  $\mu_v$ , respectively,  $\mu_c$ , and naturally ensures that mutation transitions do not reduce  $v$  or  $c$  below zero (boundary condition at  $v = 0$ ,  $c = 0$ ).

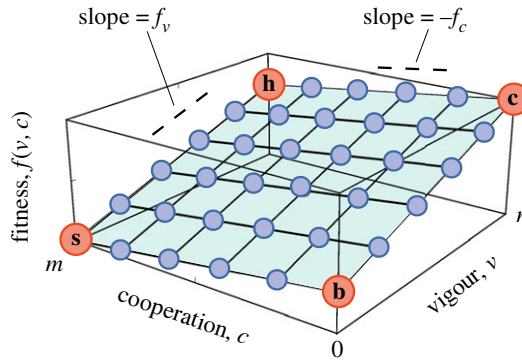


**Figure 2.** Fitness (competition) landscape for different cell types. Senescent cells are non-competitive with  $f(0, m) = 0$ . Healthy cells are moderately competitive with  $f(n, m) = f_0(1 - k)$ , while cancer cells are the most competitive species with  $f(n, 0) = f_0$ . In the model, it is important that  $\partial f / \partial v > 0$  but  $\partial f / \partial c < 0$ , i.e. the fitness landscape is tilted in favour of cancerous types. This condition ensures that loss of cooperation in the form of cheating corresponds to an advantage in selection. Parameters:  $k = 0.3$ .

### (c) Time evolution of cell fractions

To solve the master equation (2.3a), we need to specify a closure relation for  $f(v, c)$ . This procedure is analogous to path or contextual analysis of the Price equation [37], where fitness, or other parameters entering the Price equation, are partitioned into separate causes through regression equations [29–31]. In the simplest setting, we assume a linear relationship for  $f(v, c)$  (corresponding to a one-term Taylor expansion) by imposing two minimal requirements:  $f$  should increase with increasing  $v$ , and decrease with increasing  $c$ , i.e.

$$\frac{\partial f}{\partial v} > 0, \quad \frac{\partial f}{\partial c} < 0. \quad (2.4)$$

In figure 2, we depict the relative fitness of the different cell types: senescent cells (s) have the lowest fitness with  $f = 0$ , cancer cells (c) have the highest fitness  $f_0$ , while healthy cells have an intermediate fitness  $f = f_0(1 - k)$ , where  $k \in [0, 1]$  is the cost of cooperation. A linear fitness function that satisfies these requirements can then be written as  $f(v, c) = f_0k + f_v v - f_c c$ , where  $f_v = f_0(1 - k)/n$  and  $f_c = f_0k/m$ , such that  $f(n, m) = f_0(1 - k)$ ,  $f(n, 0) = f_0$ ,  $f(0, m) = 0$  and  $f(0, 0) = f_0k$ . We see that cells that have higher vigour or invest a smaller fraction of their resources on sustaining the organism have an advantage in selection compared with less vigorous or more cooperative types.

With the simple choice in equation (2.4), the master equation (2.3a) can now be solved using the method of generating functions [34] to obtain an exact analytical solution for the evolution of the population fractions of cells. To solve equation (2.1), we introduce the generating function

$$C(z, y, t) = \sum_{v,c} z^v y^c N(v, c, t), \quad (2.5)$$

and note that

$$N(t) = \sum_{v,c} N(v, c, t) = C(z, y, t) \Big|_{z=y=1} \quad (2.6)$$

and

$$N(v, c, t) = \frac{1}{v! c!} \frac{\partial^{v+c}}{\partial z^v \partial y^c} C(z, y, t) \Big|_{z=y=0}. \quad (2.7)$$

First, we multiply both sides of equation (2.1) with  $z^v y^c$  and sum over  $v$  and  $c$  to yield a single partial differential equation for the generating function  $\mathcal{C}$

$$\frac{\partial \mathcal{C}}{\partial t} = f_0 k \mathcal{C} + [\mu_v(1-z) + f_v z] \frac{\partial \mathcal{C}}{\partial z} + [\mu_c(1-y) - f_c y] \frac{\partial \mathcal{C}}{\partial y}. \quad (2.8)$$

Then, we use the method of characteristics to solve equation (2.8) subject to the initial condition that only healthy cells are present initially  $N(v, c, t=0) = N_0 \delta_{v,n} \delta_{c,m}$ , i.e.

$$\mathcal{C}(z, y, t=0) = N_0 z^n y^m, \quad (2.9)$$

yielding

$$\mathcal{C}(z, y, t) = N_0 e^{(f_h - n\mu_v - m\mu_c)t} \left[ z + \frac{\mu_v(1 - e^{(\mu_v - f_v)t})}{f_v - \mu_v} \right]^n \left[ y - \frac{\mu_c(1 - e^{(\mu_c + f_c)t})}{f_c + \mu_c} \right]^m, \quad (2.10)$$

where  $f_h = f_0(1-k)$ . The total number of cells is obtained by evaluating  $\mathcal{C}$  at  $z = y = 1$  (see (2.6))

$$\begin{aligned} N(t) &= \mathcal{C}(z, y, t)|_{z=y=1} \\ &= N_0 e^{(f_h - n\mu_v - m\mu_c)t} \left[ 1 + \frac{\mu_v(1 - e^{(\mu_v - f_v)t})}{f_v - \mu_v} \right]^n \left[ 1 - \frac{\mu_c(1 - e^{(\mu_c + f_c)t})}{f_c + \mu_c} \right]^m. \end{aligned} \quad (2.11)$$

To find the number of cells of type  $(v, c)$ , we take derivatives of  $\mathcal{C}$  evaluated at  $z = y = 0$  (see (2.7)), yielding

$$\begin{aligned} N(v, c, t) &= \frac{1}{v! c!} \frac{\partial^{v+c}}{\partial z^v \partial y^c} \mathcal{C}(z, y, t)|_{z=y=0} \\ &= N_0 e^{(f_h - n\mu_v - m\mu_c)t} \binom{n}{v} \left[ \frac{\mu_v(1 - e^{(\mu_v - f_v)t})}{f_v - \mu_v} \right]^{n-v} \binom{m}{c} \left[ \frac{\mu_c(e^{(\mu_c + f_c)t} - 1)}{f_c + \mu_c} \right]^{m-c}, \end{aligned} \quad (2.12)$$

where  $\binom{n}{v} = n!/[v!(n-v)!]$  is the binomial coefficient. Dividing (2.12) by (2.11), we obtain the fraction of cells in state  $(v, c)$  as

$$\rho(t, v, c) = \frac{N(v, c, t)}{N(t)} = \text{Bin}(v, n, p_v(t)) \text{Bin}(c, m, p_c(t)). \quad (2.13a)$$

Here,  $\text{Bin}(v, n, p) = \binom{n}{v} p^v (1-p)^{n-v}$  denotes the binomial distribution and the functions  $p_v(t)$  and  $p_c(t)$  are given by

$$p_v(t) = \frac{f_v - \mu_v}{f_v - \mu_v e^{-t/\tau_v}} \quad (2.13b)$$

and

$$p_c(t) = \frac{f_c + \mu_c}{f_c + \mu_c e^{t/\tau_c}}, \quad (2.13c)$$

where  $\tau_v = 1/(f_v - \mu_v)$  and  $\tau_c = 1/(f_c + \mu_c)$  are the two natural timescales that control the dynamics in our model. The analytical solution reveals that  $\rho(t, v, c)$  is the product of two independent binomial distributions in vigour and cooperation spaces, with  $p_v(t)$  and  $p_c(t)$  representing the (time-dependent) probabilities of cells having one unit of vigour or cooperation, respectively.

Figure 3a illustrates the time evolution of the various cell fractions for  $n = m = 1$ . This corresponds to a four-state model where cells can be in one of four states at time  $t = 0$ : healthy ( $h, (v, c) = (1, 1)$ ), senescent ( $s, (v, c) = (0, 1)$ ), cancerous ( $c, (v, c) = (1, 0)$ ), and both senescent and cancerous ( $b, (v, c) = (0, 0)$ ). We also assume that  $\mu_v \gg \mu_c$  capturing the observation that only about one per cent of human genes contributes to cancer risk [38], so that  $\mu_c/\mu_v \simeq 10^{-2}$ .

The separation of timescales between senescence-causing and cancer-causing mutations implied by  $\mu_v \gg \mu_c$  causes the resulting complex ageing dynamics to display two stages of kinetics, as reflected by the distinct timescales controlling the time evolution of the probabilities  $p_v$  and  $p_c$  (figure 3b). Initially, there is a phase of characteristic timescale  $\tau_v$  where a build-up

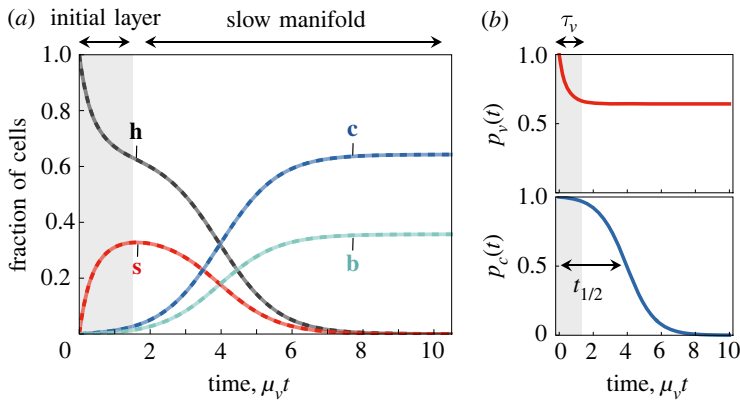


**Figure 3.** Dynamics of multicellular ageing. (a) Time evolution of fractions of healthy (*h*), senescent (*s*), cancerous (*c*) and both senescent and cancerous (*b*) cells obtained as solution to the master equation (equation (2.3a)) for  $k = 0.3$ ,  $\mu_v = 10^{-3}$ ,  $\mu_c = 10^{-5}$ ,  $f_0 = 0.004$  and  $n = m = 1$  (four-state model). Solid lines indicate the numerical solution to equation (2.3a), while dashed lines indicate the exact analytical solution (given by equation (2.13)) for initial conditions associated with  $(v, c) = (1, 1), (0, 1), (1, 0), (0, 0)$  corresponding to the four-state model. (b) Time evolution of the probabilities  $p_v(t)$  and  $p_c(t)$ , defined in equation (2.13), and graphical representation of the timescales  $\tau_v$  and  $t_{1/2}$ .

of senescent cells is observed as a result of accumulation of senescence-causing mutations. In this rapidly varying initial phase, a rapid pre-equilibrium is established between healthy and senescent cells, with the fraction of healthy cells pre-equilibrating at  $p_v(\infty)^n = [1 - \mu_v/(kf_0)]^n$  and the fraction of senescent cells approaching the maximal value  $[\mu_v/(kf_0)]^n$ . This pre-equilibrium reflects the interplay between selection  $kf_0$  and mutation forces  $\mu_v$ ; stronger competition eliminates senescent cells more effectively via natural selection hence increasing the pre-equilibrium fraction of healthy cells. During this stage of dynamics, degradation events causing cancer are negligible at leading order (i.e.  $p_c \simeq 1$ ) and the fraction of cancerous cells stays close to zero. After this rapid initial phase, the solution develops into a second, slower phase (corresponding to the slow manifold [39]), where senescent cells are slowly removed by the combined action of selection and cancer-causing mutations and the fraction of cancerous types is seen to increase with time. Cancerous cells display sigmoidal kinetics, increasing slowly initially then more rapidly and eventually reaching a plateau. At the end of this second phase of dynamics, the fractions of healthy and senescent cells approach zero, while *c* and *b* cells form an equilibrium with fractions  $[1 - \mu_v/(kf_0)]^n$  and  $[\mu_v/(kf_0)]^n$ , respectively. A measure of the characteristic timescale of cancer development is given by the time needed for  $p_c(t)$  to drop by a factor of two (the half-life), yielding  $t_{1/2} = \tau_c \ln(2 + f_c/\mu_c)$ , i.e. it is directly proportional to  $\tau_c$  with a logarithmic correction that depends on the ratio  $f_c/\mu_c$ . The half-life  $t_{1/2}$  increases with decreasing  $f_c$  or  $\mu_c$ . In particular, for  $\mu_c \rightarrow 0$ , we find  $t_{1/2} \rightarrow \infty$ , suggesting that in the absence of cancer-causing mutations, intercellular competition is able to maintain the pre-equilibrium between healthy and senescent cells indefinitely. In reality, for any value of  $\mu_c > 0$ , however small, the final ( $t \rightarrow \infty$ ) state of the system consists of an equilibrium between *c* and *b* cells and no healthy cells, in line with the idea that above some threshold age, the mortality rate monotonically increases with time [14].

#### (d) Organismal vitality, lifespan and optimal competition

With an understanding of the population dynamics using our master equation formalism, we now turn to question the relative importance of the various ‘microscopic’ (cell-level) processes and their contribution to ‘macroscopic’ (organism-level) observables, such as organismal vitality and lifespan.

To do so, a natural definition of a minimal model of average organismal vitality is the population-weighted average [14]

$$\bar{V}(t) \equiv \sum_{v,c} V(v,c) \rho(v,c,t), \quad (2.14)$$

where  $V(v,c)$  describes the contribution of cell type  $(v,c)$  to the vitality of the whole organism. Since vitality requires cells to be both vigorous and cooperative, a simple choice for  $V(v,c)$  is

$$V(v,c) = V_0 v c, \quad (2.15)$$

where  $vc$  measures the amount of resources devoted to cooperative activities and  $V_0$  is a pre-factor that sets the units of vitality. This multiplicative choice is guided by the thought that for a multicellular organism to be vital, we need cells to be both vigorous and cooperative. Since the mean of the binomial distribution  $\text{Bin}(v,n,p)$  is  $\bar{v} = np$ , for this choice of  $V(v,c)$ , the average vitality takes the simple form  $\bar{V}(t) = V_0 \bar{v}(t) \bar{c}(t) = V_0 n m p_v(t) p_c(t)$ .

Using the analytical solution for  $\rho(v,c,t)$  given by [2.13] we optimize  $\bar{V}(T)$  with respect to the strength of intercellular competition  $f_0$ , for times  $T \gg 1/f_0, 1/\mu_v$ , i.e. much larger than the timescales of proliferation and mutation (the dependence of the results on the choices of these parameters is considered in appendix B). Figure 4a shows a plot of the average organismal vitality  $\bar{V}(T)$  at the observation time  $T = 3\mu_v^{-1}$  as a function of the cost of cooperation  $k$  and the strength of competition  $f_0$ . We see that  $\bar{V}$  has a non-monotonic behaviour with  $f_0$ . In figure 4b, we show the distinct maximum of vitality as a function of the base level of competition characterized by  $f_0$  and the cost of cooperation  $k$ , characterized by an optimal curve  $f_0^*(k)$  (see appendix B and figure 5 for asymptotic analytical expressions for this optimal line  $f_0^*(k)$ ). Inspection of figure 4b shows that when  $k=0$  the optimal strength of competition diverges, i.e.  $f_0^* \rightarrow \infty$ . This is intuitive since for  $k=0$  there is no cost for cooperation. Cancer and healthy cells have therefore the same fitness, which implies that cheating gives cancer cells no advantage in selection. As we increase the cost of cooperation,  $k$ , the optimal competition  $f_0^*(k)$  gradually decays indicating that the system cannot tolerate high levels of intercellular competition when the cost of cooperation becomes large. Eventually,  $f_0^*(k)$  becomes zero at a critical value  $k = k_{\text{crit}}$  and then stays identically zero for larger values  $k > k_{\text{crit}}$ . In this limit, the fitness of healthy cells is so low that any non-zero amount of intercellular competition will result in a dominance of cancer. The critical  $k_{\text{crit}}$  depends on a combination of the rates of mutation (see appendix B for the exact analytical expression for  $k_{\text{crit}}$ ). When  $\mu_v/\mu_c \rightarrow 0$  the critical  $k_{\text{crit}} \rightarrow 0$ , while for  $\mu_v/\mu_c \rightarrow \infty$  we have  $k_{\text{crit}} \rightarrow 1$ . When  $\mu_v/\mu_c \rightarrow 1$  we find  $k_{\text{crit}} \rightarrow 1/2$ . We note that the level of optimal competition also depends on the rates of mutations causing senescence  $\mu_v$  and cancer  $\mu_c$  and on the observation time  $T$  (figure 6). Increasing  $\mu_v$  requires a higher optimal level of competition to counteract the stronger tendency of senescent cell accumulation, while increasing  $\mu_c$  causes  $f_0^*$  to decrease since the system is more susceptible to cheating. Larger times  $T$  require a lower level of intercellular competition, reflecting a balance between shorter-term advantage of cheating and longer-term detrimental effects of cheating on organismal vitality.

The sensitivity of the value of the optimal competition is defined by the derivative of the optimal line  $f_0^*(k)$  with respect to the cost of cooperation  $k$ , i.e.  $|\partial f_0^*/\partial k|$ . High sensitivity means that optimal competition is easily affected by changes in  $k$ , i.e. small fluctuations in  $k$  will push the system away from the optimum. By contrast, low sensitivity implies that optimal competition is relatively insensitive to the choice of  $k$ , which facilitates a robust approach to the optimum. In figure 4c, we show that to optimize vitality while maintaining low sensitivity a plausible solution is to operate in the regime of low to moderate  $k$ , as this choice yields a robust strategy with relatively high vitality.

To understand the dynamics of the populations as a function of the level of competition, we note that in figure 4b, the optimal curve  $f_0^*(k)$  divides  $(k, f_0)$ -space into two separate regions, which we term the *senescent* region and the *cancerous* region. As shown in figure 4d, choosing the parameters  $(k, f_0)$  along the optimal curve (scenario O) delays the loss of organismal vitality, corresponds to a balance between senescence cell accumulation and cancer proliferation.



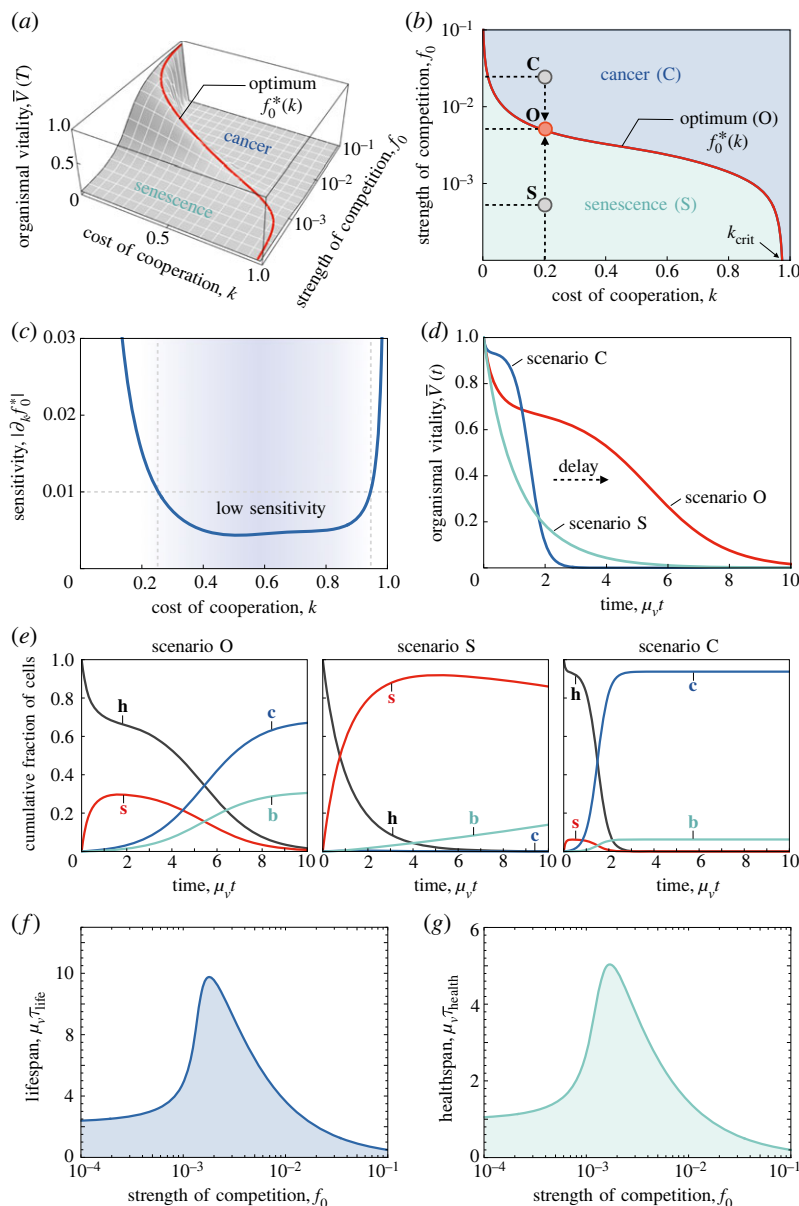


**Figure 4.** Organismal vitality and optimal competition. (a) Average organismal vitality  $\bar{V}(T)$  at observation time  $T = 3\mu_v^{-1}$  plotted against the cost of cooperation  $k$  and the strength of cellular competition  $f_0$ . The solid line indicates the position of the optimum line  $f_0^*(k)$ . The plot is obtained by numerical integration of equation (2.3a) using the same parameters as in figure 3a. (b) Optimal competition  $f_0^*(k)$  in terms of  $k$  (this corresponds to a top view of (a)). Points on the optimal line  $f_0^*(k)$  (scenario O) balance the accumulation of senescent cells and development of cancer. Points in the  $(k, f_0)$ -diagram that deviate from the optimal line (scenarios S and C) correspond to systems that are either dominated by senescence or cancer. The parameters for the different scenarios are:  $k = 0.2, f_0 = 0.004$  (O),  $f_0 = 0.02$  (S) and  $f_0 = 0.0004$  (C). (c) Sensitivity of optimal conditions, defined as  $|\partial f_0^* / \partial k|$ . The plot is obtained by numerically evaluating the derivative of the optimal line  $f_0^*(k)$  of (b) along  $k$ . Regions of low sensitivity facilitate a robust approach to optimal conditions. (d) Time evolution of average organismal vitality  $\bar{V}(t)$  for the scenarios O, S and C defined in (b). (e) Organismal lifespan  $\tau_{\text{life}}$  (defined as  $\bar{V}(\tau_{\text{life}}) = V_c$ ) as a function of strength of competition  $f_0$ . (f) Healthspan  $\tau_{\text{health}}$  (defined as  $\tau_{\text{health}} = \int_0^\infty t\bar{V}(t) dt / \int_0^\infty \bar{V}(t) dt$ ) as a function of the strength of competition  $f_0$ . Both were calculated using the same parameters as in (d) with  $V_c = 0.1$  (g) Fractions of healthy, senescent and cancerous cell types ( $h, s, c$  and  $b$ ) corresponding to scenarios O (left), S (middle) and C (right). The optimal scenario O balances senescent cell accumulation and cancer cell proliferation.

Compared with this situation, when parameters are chosen in the senescent region (scenario S) the loss of organismal vitality is dominated by accumulation of senescent cells (figure 4e), while in the cancerous region (scenario C) loss of vitality is driven by the proliferation of cancer cells (figure 4e).

In addition to determining the strength of intercellular competition that optimizes vitality, we ask how organismal lifespan or healthspan depends on intercellular competition. A measure of organismal lifespan may be defined as the time  $\tau_{\text{life}}$  at which organismal vitality falls below a fixed threshold value  $V_c$ , i.e.  $\bar{V}(t = \tau_{\text{life}}) = V_c$ . In figure 4f, we see that  $\tau_{\text{life}}$  displays a maximum with strength of competition. An alternative possibility is to account for quality of lifespan, e.g. the healthspan, via an integrated measure of vitality, which we define as  $\tau_{\text{health}} = \int_0^\infty t \bar{V}(t) dt / \int_0^\infty \bar{V}(t) dt$  (figure 4g), a quantity that characterizes the (scaled) first moment of the average organismal vitality.

### 3. Discussion

In this study, we have proposed a model for ageing in terms of the dynamics of a multicellular population characterized by its vigour and cooperation, and a fitness parameter that is a function of these variables. Using a master-equation-based framework, we derived a replicator-like dynamical equation accounting for fluxes due to mutations that lead to cancer and senescence. Assuming a minimal closure relation for the fitness that is linear in the vigour and cooperation, we are led to an analytic solution for the evolution of the relative fraction of healthy, senescent and cancerous populations while accounting for the interplay between competition and cooperation. Using our model and a simple choice of organismal vitality that is multiplicative in the vigour and cooperation, we then probed the optimal level of intercellular competition that maximizes organismal vitality, balancing the cost of cooperation and the strength of competition.

Our study shows that for multicellular ageing, too little competition is a losing strategy because it leads to senescent cell accumulation. On the other hand, too much competition is also a losing strategy because even if senescent cells are eliminated it leads to cheater-cell proliferation in the long term. This is reminiscent of Parrondo's paradox as highlighted in a commentary [27], wherein periodic and stochastic switching between two losing strategies may lead to a winning strategy [40–43]. This idea has been invoked in a range of biological systems to explain adaptation in areas ranging from genetics to ecology [44–46]. Following the logic of Parrondo's paradox suggests that a potentially fruitful approach to delay multicellular ageing could combine both (losing) strategies to achieve a fine balance that delays senescence and staves off cancer. In this optimal scenario, competition is strategically reduced when cheater cells over-proliferate and increased back when senescent cells over-accumulate. A similar strategy may be realized with coexisting subpopulations of uncompetitive and competitive cells if the ratio between the subpopulations is strategically changed in response to the changing environment.

Our framework may be extended in multiple ways. Effective multicellularity not only requires cooperation between cells, but also mechanisms for suppressing conflict that result from it. This effect may be accounted for by introducing a feedback between strength of competition and the current system state. To investigate the impact of drugs that clear senescent or cancer cells [47], we can envisage coupling the master replicator equation with dynamic equations for an inhibitor that removes deleterious cell types. Generalizing our results could thus provide a framework for interrogating the effect of strategies to combat ageing and cancer dynamics and how to optimize them. Furthermore, our model considers detrimental mutations reducing vigour or cooperation as irreversible. Even though proliferation arrest in senescence cells is essentially irreversible, certain biological manipulations, including inactivation of specific tumour suppressor genes, can reverse senescence [48]. The latter scenario could be studied by making transitions between cell types in our model reversible, and more generally by including separate dynamic equations modelling changes of  $v$  and  $c$  over evolutionary timescales to model the effect of tumour suppressor genes. While we have limited ourselves here to the balance between cooperation and competition during the later stages of life associated with ageing, similar questions arise

during the developmental stages of organisms when proliferation rates of cells are high and thus susceptible to mutational errors [49]. Understanding the dynamic regulation (and misregulation) of intercellular competition in early development might also be amenable to our approach.

Although we have limited ourselves to studying the role of discrete mutations, it is not hard to generalize our framework to the case of continuously varying vigour and cooperation. This leads to a Boltzmann-like equation for the dynamics of cellular populations (see appendix C). Finally, it is worth noting the natural appearance of extensive variables such as vigour (and vitality) and intensive variables such as cooperation (and competition), suggesting natural analogies to (non-equilibrium) thermodynamics. The relation between these variables and various forms of closure relations will be explored in a separate study.

**Data accessibility.** This article has no additional data.

**Declaration of AI use.** We have not used AI-assisted technologies in creating this article.

**Authors' contributions.** T.C.T.M.: conceptualization, data curation, formal analysis, funding acquisition, investigation, methodology, project administration, validation, visualization, writing—original draft, writing—review and editing; L.M.: conceptualization, formal analysis, funding acquisition, investigation, methodology, project administration, validation, writing—original draft, writing—review and editing.

Both authors gave final approval for publication and agreed to be held accountable for the work performed therein.

**Conflict of interest declaration.** We declare we have no competing interests.

**Funding.** No funding has been received for this article.

**Acknowledgements.** We acknowledge support from the Swiss National Science Foundation (T.C.T.M.), Peterhouse, Cambridge (T.C.T.M.), the Simons Foundation (L.M.) and the Henri Seydoux Fund (L.M.).

## Appendix A. Master-equation formalism for the Price equation

In this appendix, we first derive the Price equation [29,30] from a master equation perspective [34]. This formalism will provide the basis for deriving, in appendix A(d), the master equation of multicellular ageing (equations (2.1) and (2.3a) of the main text).

### (a) Kinetic equation for cell populations

Consider a system of cell types described by the multi-index

$$\underline{i} = (i_1, i_2, \dots, i_n),$$

in an  $n$ -dimensional coordinate system. For instance, in our model of multicellular ageing, we set  $\underline{i} = (v, c)$  where  $v$  is cell vigour and  $c$  is cell cooperation, see appendix A(d). Let  $N(\underline{i}, t)$  be the number of cells of type  $\underline{i}$  at time  $t$ .  $N(\underline{i}, t)$  evolves in time as a result of two effects: (i) growth and (ii) somatic mutations.

- **Growth.** We define the relative growth probability per developmental time step  $\Delta t$  of the population of cells of type  $\underline{i}$  as

$$w(\underline{i}) = \frac{N(\underline{i}, t + \Delta t)}{N(\underline{i}, t)}. \quad (\text{A } 1)$$

As we will quantify, differences in growth rates are the basis of selection: the species that grow faster have an advantage during selection over the species that grow more slowly [29,30].

- **Somatic mutations.** In addition to growth, individual cell populations are subject to somatic mutations. These are permanent changes of cell type, i.e. changes of  $\underline{i}$  to some other type  $\underline{j}$ . We let  $\pi(\underline{j} \rightarrow \underline{i})$  be the probability of a mutation that switches type from  $\underline{j}$  to  $\underline{i}$  in time step  $\Delta t$ .

Then the dynamics of  $N(\underline{i}, t)$  are given by combining the effects of growth and selection and is given by

$$N(\underline{i}, t + \Delta t) = w(\underline{i}) N(\underline{i}, t) + \sum_{\underline{j} \neq \underline{i}} \pi(\underline{j} \rightarrow \underline{i}) N(\underline{j}, t) - \sum_{\underline{j} \neq \underline{i}} \pi(\underline{i} \rightarrow \underline{j}) N(\underline{i}, t). \quad (\text{A } 2)$$

This equation can be re-written as

$$N(\underline{i}, t + \Delta t) - N(\underline{i}, t) = (w(\underline{i}) - 1) N(\underline{i}, t) + \sum_{\underline{j}} [\pi(\underline{j} \rightarrow \underline{i}) N(\underline{j}, t) - \pi(\underline{i} \rightarrow \underline{j}) N(\underline{i}, t)]. \quad (\text{A } 3)$$

We now take the continuum-time limit in (A 3) by letting  $\Delta t \rightarrow 0$  and using

$$N(\underline{i}, t + \Delta t) - N(\underline{i}, t) \simeq \frac{\partial N(\underline{i}, t)}{\partial t} \Delta t.$$

This yields a master equation (with continuous time) for the populations of cells in state  $\underline{i}$

$$\begin{aligned} \frac{\partial N(\underline{i}, t)}{\partial t} &= f(\underline{i}) N(\underline{i}, t) \\ &+ \sum_{\underline{j}} [\mu(\underline{j} \rightarrow \underline{i}) N(\underline{j}, t) - \mu(\underline{i} \rightarrow \underline{j}) N(\underline{i}, t)], \end{aligned} \quad (\text{A } 4a)$$

where

$$f(\underline{i}) = \lim_{\Delta t \rightarrow 0} \frac{w(\underline{i}) - 1}{\Delta t}, \quad (\text{A } 4b)$$

is the growth rate and

$$\mu(\underline{j} \rightarrow \underline{i}) = \lim_{\Delta t \rightarrow 0} \frac{\pi(\underline{j} \rightarrow \underline{i})}{\Delta t}, \quad (\text{A } 4c)$$

is the rate of mutation. The first term in (A 4) describes the (exponential) growth of the population of cell type  $\underline{i}$  with growth rate  $f(\underline{i})$ ; the second term in (A 4) describes mutations of type  $\underline{i}$  into any other type  $\underline{j}$ , while the third term in (A 4) describes the increase of population of type  $\underline{i}$  as a result of mutations from any type  $\underline{j}$  into  $\underline{i}$ .

## (b) Kinetic equations for fractions

We now consider the dynamics of the fraction of cells of type  $\underline{i}$ , which is defined as

$$\rho(\underline{i}, t) = \frac{N(\underline{i}, t)}{N(t)}, \quad (\text{A } 5a)$$

where

$$N(t) = \sum_{\underline{i}} N(\underline{i}, t), \quad (\text{A } 5b)$$

is the total population.

### (i) Dynamics of total population

To obtain a dynamical equation for  $N(t)$ , we sum (A 4) over  $\underline{i}$ , yielding

$$\begin{aligned} \frac{dN(t)}{dt} &= \sum_{\underline{i}} \frac{\partial N(\underline{i}, t)}{\partial t} \\ &= \sum_{\underline{i}} f(\underline{i}) N(\underline{i}, t) + \sum_{\underline{i}, \underline{j}} [\mu(\underline{j} \rightarrow \underline{i}) N(\underline{j}, t) - \mu(\underline{i} \rightarrow \underline{j}) N(\underline{i}, t)] \\ &= \left( \sum_{\underline{i}} f(\underline{i}) \rho(\underline{i}, t) \right) N(t) + \underbrace{\sum_{\underline{i}, \underline{j}} [\mu(\underline{j} \rightarrow \underline{i}) \rho(\underline{j}, t) - \mu(\underline{i} \rightarrow \underline{j}) \rho(\underline{i}, t)]}_{=0} N(t) \\ &= \left( \sum_{\underline{i}} f(\underline{i}) \rho(\underline{i}, t) \right) N(t). \end{aligned} \quad (\text{A } 6)$$

Thus,

$$\frac{dN(t)}{dt} = \bar{f}(t) N(t), \quad (\text{A } 7)$$

where

$$\bar{f}(t) = \sum_{\underline{i}} f(\underline{i}) \rho(\underline{i}, t), \quad (\text{A } 8)$$

is the average growth rate (of the population), i.e. the total number of cells grows according to the average growth rate.

### (ii) Dynamics of cell fractions

The dynamic equations for the fractions  $\rho(\underline{i}, t)$  are obtained from (A 5) by applying the chain rule for derivatives

$$\frac{\partial \rho(\underline{i}, t)}{\partial t} = \frac{1}{N(t)} \frac{\partial N(\underline{i}, t)}{\partial t} - \frac{N(\underline{i}, t)}{N(t)^2} \frac{dN(t)}{dt}. \quad (\text{A } 9)$$

Together with (A 4) and (A 7), this yields

$$\frac{\partial \rho(\underline{i}, t)}{\partial t} = \overbrace{(f(\underline{i}) - \bar{f}(t)) \rho(\underline{i}, t)}^{\text{selection (competition)}} + \overbrace{\sum_{\underline{j}} [\mu(\underline{j} \rightarrow \underline{i}) \rho(\underline{j}, t) - \mu(\underline{i} \rightarrow \underline{j}) \rho(\underline{i}, t)]}_{\text{somatic mutations}}. \quad (\text{A } 10)$$

(A 10) has two contributions. The first term in (A 10) describes the effect of selection: cell types that with growth rate faster than the average ( $f(\underline{i}) > \bar{f}$ ) will be selected over many generations, while slowly reproducing types will be left behind. The second contribution to (A 10) describes the effect of somatic mutations, which is captured by means of reaction fluxes into and away from the population of type  $\underline{i}$ .

### (iii) Conservation of total fraction

We note that

$$\begin{aligned} \frac{d}{dt} \left( \sum_{\underline{i}} \rho(\underline{i}, t) \right) &= \sum_{\underline{i}} \frac{\partial \rho(\underline{i}, t)}{\partial t} \\ &= \sum_{\underline{i}} (f(\underline{i}) - \bar{f}(t)) \rho(\underline{i}, t) + \sum_{\underline{i}, \underline{j}} [\mu(\underline{j} \rightarrow \underline{i}) \rho(\underline{j}, t) - \mu(\underline{i} \rightarrow \underline{j}) \rho(\underline{i}, t)] \\ &= 0, \end{aligned} \quad (\text{A } 11)$$

which corresponds to the conservation law

$$\sum_i \rho(\underline{i}, t) = 1. \quad (\text{A } 12)$$

### (c) Price equation

We now derive the Price equation from (A 10). The Price equation is a dynamical equation for the average of some trait  $z(\underline{i})$  of the population. The mean trait is defined as

$$\bar{z}(t) = \sum_i z(\underline{i})\rho(\underline{i}, t). \quad (\text{A } 13)$$

A dynamic equation for  $\bar{z}$  can be obtained by multiplying (A 10) by  $z(\underline{i})$  on both sides and summing over all possible cell types  $\underline{i}$ , yielding

$$\begin{aligned} \frac{d\bar{z}(t)}{dt} &= \sum_i z(\underline{i}) \frac{d\rho(\underline{i}, t)}{dt} = \sum_i z(\underline{i})f(\underline{i})\rho(\underline{i}, t) - \bar{z}(t)\bar{f}(t) \\ &\quad + \sum_{\underline{i}\underline{j}} z(\underline{i})\mu(\underline{j} \rightarrow \underline{i})\rho(\underline{j}, t) - \sum_{\underline{i}\underline{j}} z(\underline{i})\mu(\underline{i} \rightarrow \underline{j})\rho(\underline{i}, t). \end{aligned} \quad (\text{A } 14)$$

After swapping indices  $\underline{i}$  and  $\underline{j}$  in the double-sums, we find

$$\frac{d\bar{z}(t)}{dt} = \sum_i z(\underline{i})f(\underline{i})\rho(\underline{i}, t) - \bar{z}(t)\bar{f}(t) + \sum_i \rho(\underline{i}, t) \sum_{\underline{j}} [z(\underline{j}) - z(\underline{i})]\mu(\underline{i} \rightarrow \underline{j}). \quad (\text{A } 15)$$

The first two terms can be recognized as the covariance  $\sum_i z(\underline{i})f(\underline{i})\rho(\underline{i}, t) - \bar{z}(t)\bar{f}(t) = \text{cov}(z, f)$ , such that we arrive at the Price equation

$$\frac{d\bar{z}(t)}{dt} = \text{cov}(z, f) + \bar{\Delta z}(t), \quad (\text{A } 16a)$$

where

$$\begin{aligned} \Delta z(\underline{i}) &= \sum_{\underline{j}} [z(\underline{j}) - z(\underline{i})]\mu(\underline{i} \rightarrow \underline{j}) \\ &= \mu \left( \sum_{\underline{j}} z(\underline{j}) \frac{\mu(\underline{i} \rightarrow \underline{j})}{\mu} - z(\underline{i}) \right), \end{aligned} \quad (\text{A } 16b)$$

with  $\mu = \sum_{\underline{j}} \mu(\underline{i} \rightarrow \underline{j})$ . The term  $\Delta z(\underline{i})$  has an intuitive interpretation: it is the difference between the value of  $z$  for type  $\underline{i}$  and the average of other species weighted over the mutation distribution. Thus the Price equation (A 16) describes the time evolution of the average value of  $z$  as a result of natural selection (first term, covariance term) and mutations (second term), derived from a master equation formalism.

### (d) Master-equation for multicellular ageing

We now apply the formalism of appendix A(a)–(c) to construct a master equation description of multicellular ageing. We describe cell types by means of two traits, vigour  $v$  and cooperation  $c$ , which define a two-dimensional coordinate system

$$\underline{i} = (v, c).$$

As discussed in [14], we assume that somatic mutations affect only one cellular trait at a time and in a single step, either vigour with rate  $\mu_v(v)$  or cooperation with rate  $\mu_c(c)$ .

### (i) Cell populations

Using (A 4), we obtain the following master equation for cell populations:

$$\begin{aligned} \frac{\partial N(v, c, t)}{\partial t} = & f(v, c)N(v, c, t) \\ & + \mu_v(v+1)N(v+1, c, t) - \mu_v(v)N(v, c, t) \\ & + \mu_c(c+1)N(v, c+1, t) - \mu_c(c)N(v, c, t). \end{aligned} \quad (\text{A } 17)$$

This is equation (2.1) of the main text.

### (ii) Cell fractions

Using (A 10), we obtain the following master equation for cell fractions:

$$\begin{aligned} \frac{\partial \rho(v, c, t)}{\partial t} = & (f(v, c) - \bar{f}(t))\rho(v, c, t) \\ & + \mu_v(v+1)\rho(v+1, c, t) - \mu_v(v)\rho(v, c, t) \\ & + \mu_c(c+1)\rho(v, c+1, t) - \mu_c(c)\rho(v, c, t), \end{aligned} \quad (\text{A } 18a)$$

where

$$\bar{f}(t) = \sum_{v,c} f(v, c) \rho(v, c, t), \quad (\text{A } 18b)$$

is the average competition. This is equation (2.3a) of the main text.

## Appendix B. Optimal competition

Here, we derive asymptotic analytical expressions for the optimal competition  $f_0^*(k)$ . We will focus on two limits: (i)  $k \rightarrow 0$  and (ii)  $f_0^* \rightarrow 0$ , which occurs at a critical  $k \rightarrow k_{\text{crit}}$  (figure 5).

### (a) Limit $k \rightarrow 0$

Consider the average vitality

$$\bar{V}(t) = V_0 n m p_v(t) p_c(t), \quad (\text{B } 1)$$

as derived in the main text. In the limit of large observation times  $T \gg \tau_v$ , the function  $p_v(t)$  has pre-equilibrated to  $1 - \mu_v/f_v$ . Moreover, for  $\mu_v \gg \mu_c$ , we neglect terms proportional to  $\mu_c$  in front of  $f_c$ . This yields

$$\bar{V}(T) = \frac{V_0 n m k}{(1-k)} \frac{(f_v - \mu_v)}{(f_c + \mu_c e^{f_c T})}, \quad (\text{B } 2)$$

where  $T$  is the observation time. We maximize (B 2) with respect to  $f_0$

$$\begin{aligned} 0 = & \frac{\partial \bar{V}(T)}{\partial f_0} \\ = & \frac{V_0 n m k}{(1-k)} \frac{(k\mu_v + \mu_c e^{f_0 k T} [(1-k)(k f_0 T - 1) - \mu_v k T])}{(f_0 k + \mu_c e^{f_0 k T})^2}. \end{aligned} \quad (\text{B } 3)$$

This yields the optimal strength of competition as

$$f_0^* = \frac{1}{kT} + \frac{\mu_v}{1-k} + \frac{W(z)}{kT} \quad \text{and} \quad z = \frac{e^{-1 - (\mu_v k T / (1-k))} k \mu_v}{(1-k) \mu_c}, \quad (\text{B } 4)$$

where  $W(z)$  is the Lambert  $W$ -function, defined by  $z = We^W$ . In the limit  $t \rightarrow \infty$ , we obtain

$$\lim_{T \rightarrow \infty} f_0^* = \frac{\mu_v}{1-k}.$$

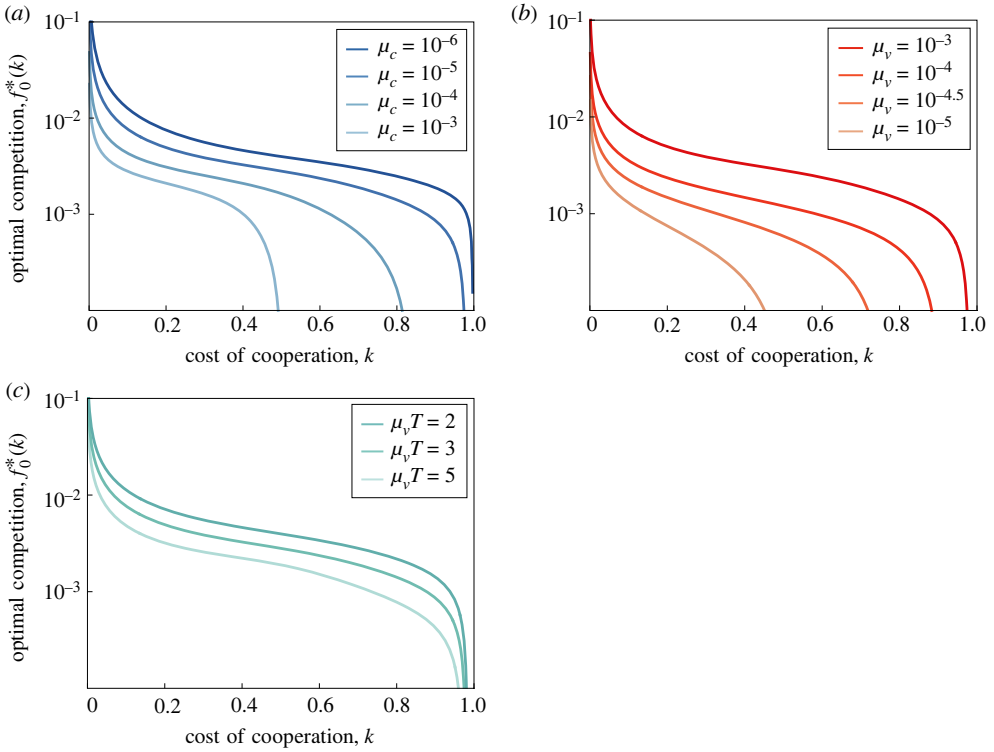


**Figure 5.** Optimal competition with varying  $\mu_v$ ,  $\mu_c$  and  $T$ . The figure shows how the optimal competition line  $f_0^*(k)$  changes with varying (a) the rate of senescence-causing mutations  $\mu_v$ , (b) the rate of cancer-causing mutations  $\mu_c$  and (c) the observation time  $T$ .

### (b) Limit $k \rightarrow k_{crit}$

As  $k \rightarrow k_{crit}$ , the optimal competition  $f_0^*$  approaches zero. To capture this behaviour, we consider the leading order terms in the Taylor expansion of  $\bar{V}(T)$  at  $f_0 = 0$  and yields

$$\bar{V}(T) = A + Bf_0 + \frac{C}{2}f_0^2 + \text{higher-order terms.} \quad (\text{B5})$$

Maximization of  $\bar{V}(T)$  with respect to  $f_0$  yields

$$0 = \frac{\partial \bar{V}(T)}{\partial f_0} = B + Cf_0 \Rightarrow f_0^* = -\frac{A}{B}. \quad (\text{B6})$$

An optimum  $f_0^* > 0$  exists when  $A > 0$ , which occurs for  $k > k_{crit}$  where

$$k_{crit} = \frac{1}{1 + ((\mu_v \mu_c T - \mu_v(1 - e^{-\mu_c T})) / (\mu_v \mu_c T - \mu_c(1 - e^{-\mu_v T})))}. \quad (\text{B7})$$

For  $k < k_{crit}$ , the optimum is  $f_0^* = 0$ .

## Appendix C. Continuum limit and the Boltzmann transport equation

### (a) Continuum limit

In the limit when the variables  $v$  and  $c$  vary continuously, we replace finite differences in (2.3a) by derivatives. In particular, for a smooth function  $\phi(v, c, t)$

$$\phi(v + dv, c, t) - \phi(v, c, t) \simeq \frac{\partial \phi(v, c, t)}{\partial v} dv \quad (\text{C1a})$$



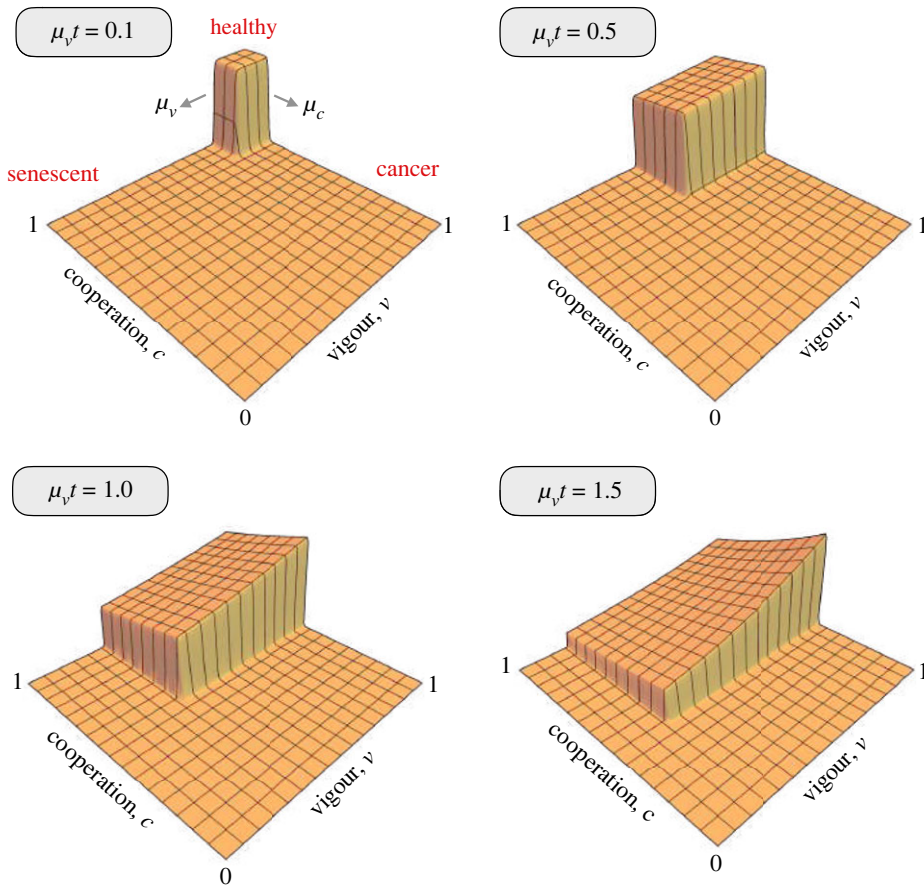


**Figure 6.** Solution to continuous master equation. The figure shows snapshots of the solution  $N(v, c, t)$  of the continuous master equation (C3) with initial profile  $N_0(v, c) = N_0 \tanh((v - v_0)/w) \tanh((c - c_0)/w)$ . The parameters are:  $\mu_v = 10^{-3}$ ,  $\mu_c = 5 \times 10^{-4}$ ,  $f_0 = 10^{-3}$ ,  $k = 0.6$ ,  $n = m = 1$ ,  $N_0 = 1$ ,  $v_0 = c_0 = 0.9$ ,  $w = 0.01$ .

and

$$\phi(v, c + dc, t) - \phi(v, c, t) \simeq \frac{\partial \phi(v, c, t)}{\partial c} dc. \tag{C1b}$$

We can thus reformulate equation (2.1) and (2.3a) as partial differential equations.

### (i) Continuous master equation for cell populations

For cell populations,  $N(t, v, c)$ , this procedure yields

$$\frac{\partial N(v, c, t)}{\partial t} = f(v, c) N(v, c, t) + \frac{\partial}{\partial v} (\mu_v(v) N(v, c, t)) + \frac{\partial}{\partial c} (\mu_c(c) N(v, c, t)). \tag{C2}$$

This can be written as

$$\frac{\partial N}{\partial t} + \nabla \cdot (\mathbf{u} N) = f N, \tag{C3}$$

where  $\mathbf{u} = (-\mu_v(v), -\mu_c(c))$  is a velocity vector in  $(v, c)$ -space and  $\nabla = (\partial_v, \partial_c)$ .

The solution to the continuous master equation (C3) can be obtained using the method of characteristics. For an initial distribution  $N(v, c, t = 0) = N_0(v, c)$  the solution is

$$N(v, c, t) = N_0(v e^{\mu_v t}, c e^{\mu_c t}) e^{(f_0 k + \mu_v + \mu_c)t} \exp \left[ \frac{v f_v (e^{\mu_v t} - 1)}{\mu_v} - \frac{c f_c (e^{\mu_c t} - 1)}{\mu_c} \right]. \tag{C4}$$

This solution is shown in figure 6 and resembles a moving front in the  $v$ - and  $c$ -directions.

## (ii) Continuous master equation for cell fractions

Introducing the total number of cells as

$$N(t) = \int N(v, c, t) \, dv \, dc, \quad (\text{C } 5)$$

we find the evolution equation

$$\frac{dN(t)}{dt} = \bar{f}(t) N(t), \quad (\text{C } 6)$$

where the average competition is

$$\bar{f}(t) = \int f(v, c) \rho(v, c, t) \, dv \, dc. \quad (\text{C } 7)$$

The equation for the cell fractions  $\rho(v, c, t) = N(v, c, t)/N(t)$  follows from applying the chain rule for derivatives

$$\frac{\partial \rho(v, c, t)}{\partial t} = \frac{1}{N(t)} \frac{\partial N(v, c, t)}{\partial t} - \frac{N(v, c, t)}{N(t)^2} \frac{dN(t)}{dt}, \quad (\text{C } 8)$$

and combining (C 2) with (C 6), yielding:

$$\frac{\partial \rho}{\partial t} - \frac{\partial(\mu_v \rho)}{\partial v} - \frac{\partial(\mu_c \rho)}{\partial c} = (f - \bar{f}(t)) \rho. \quad (\text{C } 9)$$

Not surprisingly, (C 9) is analogous to the Boltzmann transport equation (BTE)

$$\frac{\partial \rho}{\partial t} + \nabla \cdot (\mathbf{u} \rho) = (\partial_t \rho)_{\text{coll}}, \quad (\text{C } 10)$$

and suggests an analogy with kinetic gas theory. The left-hand side of (C 9) describes the evolution of a probability density due to mutational flows. The right-hand side of (C 9) is the ‘collision’ integral that characterizes changes due to interactions and is given by

$$(\partial_t \rho)_{\text{coll}} = \int (f(v, c) - f(v', c')) \rho(v, c, t) \rho(v', c', t) \, dv' \, dc'. \quad (\text{C } 11)$$

In kinetic gas theory, this term captures the forces due to particle collisions. In the context of multicellular ageing, the collision integral describes the effect of selection: cell types with low competition are ‘displaced’ by more competitive cell types who eventually take over the entire system. These two driving forces associated with selection and mutation correspond to the direct and inertial forces pointed out by Frank [30]. In particular, direct forces (collision forces) are proportional to  $f(v, c) - \bar{f}(t)$ , which in the literature is known as Fisher’s excess of fitness [30].

## (b) Continuous Price equation

We now consider the continuous analogue of the Price equation in the hydrodynamic limit treated above. We first define the average of any quantity  $\Phi(v, c)$

$$\bar{\Phi}(t) = \int \Phi(v, c) \rho(v, c, t) \, dv \, dc. \quad (\text{C } 12)$$

The time evolution of  $\Phi(v, c)$  can be obtained by differentiating (C 12) and combining it with the BTE, (C 9), a procedure that is analogous to obtaining the equations of hydrodynamics from the

BTE in kinetic theory. We have

$$\frac{d\bar{\Phi}}{dt} = \int \Phi \frac{\partial \rho}{\partial t} dv dc. \quad (\text{C } 13)$$

Inserting the evolution equation for  $\rho$ , (C9), yields using integration by parts

$$\begin{aligned} \frac{d\bar{\Phi}}{dt} &= \int \Phi (f - \bar{f}) \rho dv dc + \int \Phi \nabla \cdot (\mathbf{u} \rho) dv dc \\ &= \int \Phi f \rho dv dc - \bar{f} \int \Phi \rho dv dc - \int \nabla \Phi \cdot \mathbf{u} \rho dv dc \\ &= \overline{\Phi f} - \bar{\Phi} \bar{f} + \overline{\nabla \Phi \cdot \mathbf{u}}. \end{aligned} \quad (\text{C } 14)$$

Thus the continuum version of the Price equation (A16) reads

$$\frac{d\bar{\Phi}}{dt} = \underbrace{\overline{\Phi f} - \bar{\Phi} \bar{f}}_{\text{covariance}} + \underbrace{\overline{\nabla \Phi \cdot \mathbf{u}}}_{\text{mutations}} = \text{cov}(\Phi, f) + \overline{\nabla \Phi \cdot \mathbf{u}}. \quad (\text{C } 15)$$

This allows us to write the dynamic equations for  $\bar{v}$ ,  $\bar{c}$  and  $\bar{f}$  as

$$\frac{d\bar{v}}{dt} = \bar{v} \bar{f} - \bar{v} \bar{f} - \mu_v \bar{v}, \quad (\text{C } 16)$$

$$\frac{d\bar{c}}{dt} = \bar{c} \bar{f} - \bar{c} \bar{f} - \mu_c \bar{c} \quad (\text{C } 17)$$

and

$$\frac{d\bar{f}}{dt} = \bar{f}^2 - \bar{f}^2 + \overline{\mathbf{u} \cdot \nabla f}. \quad (\text{C } 18)$$

## References

1. Strassmann JE, Queller DC. 2010 The social organism: congresses, parties, and committees. *Evol. Int. J. Org. Evol.* **64**, 605–616. (doi:10.1111/j.1558-5646.2009.00929.x)
2. Aktipis CA, Boddy AM, Jansen G, Hibner U, Hochberg ME, Maley CC, Wilkinson GS. 2015 Cancer across the tree of life: cooperation and cheating in multicellularity. *Phil. Trans. R. Soc. B* **370**, 20140219. (doi:10.1098/rstb.2014.0219)
3. Michod RE. 2000 *Darwinian dynamics: evolutionary transitions in fitness and individuality*. Princeton, NJ: Princeton University Press.
4. Pfeiffer T, Bonhoeffer S. 2003 An evolutionary scenario for the transition to undifferentiated multicellularity. *Proc. Natl Acad. Sci. USA* **100**, 1095–1098. (doi:10.1073/pnas.0335420100)
5. Baillon L, Basler K. 2014 Reflections on cell competition. In *Seminars in cell & developmental biology*, vol. 32, pp. 137–144. Elsevier.
6. Michod RE. 1996 Cooperation and conflict in the evolution of individuality. II. Conflict mediation. *Proc. R. Soc. Lond. B* **263**, 813–822. (doi:10.1098/rspb.1996.0121)
7. Clavería C, Torres M. 2016 Cell competition: mechanisms and physiological roles. *Annu. Rev. Cell Dev. Biol.* **32**, 411–439. (doi:10.1146/annurev-cellbio-111315-125142)
8. Harman D. 1981 The aging process. *Proc. Natl Acad. Sci. USA* **78**, 7124–7128. (doi:10.1073/pnas.78.11.7124)
9. Vural DC, Morrison G, Mahadevan L. 2014 Aging in complex interdependency networks. *Phys. Rev. E* **89**, 022811. (doi:10.1103/PhysRevE.89.022811)
10. Sun ED, Michaels TC, Mahadevan L. 2020 Optimal control of aging in complex networks. *Proc. Natl Acad. Sci. USA* **117**, 20404–20410. (doi:10.1073/pnas.2006375117)
11. Taneja S, Mitnitski AB, Rockwood K, Rutenberg AD. 2016 Dynamical network model for age-related health deficits and mortality. *Phys. Rev. E* **93**, 022309. (doi:10.1103/PhysRevE.93.022309)
12. Farrell SG, Mitnitski AB, Rockwood K, Rutenberg AD. 2016 Network model of human aging: frailty limits and information measures. *Phys. Rev. E* **94**, 052409. (doi:10.1103/PhysRevE.94.052409)
13. Mitnitski A, Rutenberg A, Farrell S, Rockwood K. 2017 Aging, frailty and complex networks. *Biogerontology* **18**, 433–446. (doi:10.1007/s10522-017-9684-x)

14. Nelson P, Masel J. 2017 Intercellular competition and the inevitability of multicellular aging. *Proc. Natl Acad. Sci. USA* **114**, 12 982–12 987. (doi:10.1073/pnas.1618854114)
15. Vijg J. 2000 Somatic mutations and aging: a re-evaluation. *Mutat. Res./Fundam. Mol. Mech. Mutagen.* **447**, 117–135. (doi:10.1016/S0027-5107(99)00202-X)
16. Campisi J. 2013 Aging, cellular senescence, and cancer. *Annu. Rev. Physiol.* **75**, 685–705. (doi:10.1146/annurev-physiol-030212-183653)
17. Van Deursen JM. 2014 The role of senescent cells in ageing. *Nature* **509**, 439. (doi:10.1038/nature13193)
18. Wodarz D. 2007 Effect of stem cell turnover rates on protection against cancer and aging. *J. Theor. Biol.* **245**, 449–458. (doi:10.1016/j.jtbi.2006.10.013)
19. Biteau B, Karpac J, Supoyo S, DeGennaro M, Lehmann R, Jasper H. 2010 Lifespan extension by preserving proliferative homeostasis in *Drosophila*. *PLoS Genet.* **6**, e1001159. (doi:10.1371/journal.pgen.1001159)
20. Chalmers AD, Whitley P, Vivarelli S, Wagstaff L, Piddini E. 2012 Cell wars: regulation of cell survival and proliferation by cell competition. *Essays Biochem.* **53**, 69–82. (doi:10.1042/bse0530069)
21. Hanahan D, Weinberg RA. 2011 Hallmarks of cancer: the next generation. *Cell* **144**, 646–674. (doi:10.1016/j.cell.2011.02.013)
22. Tenen DG. 2003 Disruption of differentiation in human cancer: AML shows the way. *Nat. Rev. Cancer* **3**, 89. (doi:10.1038/nrc989)
23. Gil J, Rodriguez T. 2016 Cancer: the transforming power of cell competition. *Curr. Biol.* **26**, R164–R166. (doi:10.1016/j.cub.2016.01.006)
24. Hausser J, Alon U. 2020 Tumour heterogeneity and the evolutionary trade-offs of cancer. *Nat. Rev. Cancer* **20**, 1–11. (doi:10.1038/s41568-020-0241-6)
25. Goodell MA, Rando TA. 2015 Stem cells and healthy aging. *Science* **350**, 1199–1204. (doi:10.1126/science.aab3388)
26. Wagner GP. 2017 The power of negative [theoretical] results. *Proc. Natl Acad. Sci. USA* **114**, 12 851–12 852. (doi:10.1073/pnas.1718862114)
27. Cheong KH, Koh JM, Jones MC. 2018 Multicellular survival as a consequence of Parrondo's paradox. *Proc. Natl Acad. Sci. USA* **115**, E5258–E5259. (doi:10.1073/pnas.1806485115)
28. Mitteldorf J, Fahy GM. 2018 Questioning the inevitability of aging. *Proc. Natl Acad. Sci. USA* **115**, E558–E558. (doi:10.1073/pnas.1720331115)
29. Queller DC. 2017 Fundamental theorems of evolution. *Am. Nat.* **189**, 345–353. (doi:10.1086/690937)
30. Frank SA. 2012 Natural selection. IV. The price equation. *J. Evol. Biol.* **25**, 1002–1019. (doi:10.1111/j.1420-9101.2012.02498.x)
31. Okasha S. 2006 *Evolution and the levels of selection*. Oxford, UK: Oxford University Press.
32. Schmitt CA, Wang B, Demaria M. 2022 Senescence and cancer—role and therapeutic opportunities. *Nat. Rev. Clin. Oncol.* **19**, 619–636. (doi:10.1038/s41571-022-00668-4)
33. Promislow DE, Tatar M. 1998 Mutation and senescence: where genetics and demography meet. *Genetica* **102**, 299–314. (doi:10.1023/A:1017047212008)
34. Krapivsky PL, Redner S, Ben-Naim E. 2010 *A kinetic view of statistical physics*. Cambridge, UK: Cambridge University Press.
35. Cressman R, Tao Y. 2014 The replicator equation and other game dynamics. *Proc. Natl Acad. Sci. USA* **111**, 10 810–10 817. (doi:10.1073/pnas.1400823111)
36. Gomez K, Bertram J, Masel J. 2020 Mutation bias can shape adaptation in large asexual populations experiencing clonal interference. *Proc. R. Soc. B* **287**, 20201503. (doi:10.1098/rspb.2020.1503)
37. Li CC *et al.* 1975 *Path Analysis—a primer*. Pacific Grove, CA: The Boxwood Press.
38. Futreal PA, Coin L, Marshall M, Down T, Hubbard T, Wooster R, Rahman N, Stratton MR. 2004 A census of human cancer genes. *Nat. Rev. Cancer* **4**, 177. (doi:10.1038/nrc1299)
39. Hinch EJ. 1991 Perturbation Methods. In *Matched asymptotic expansion*, Cambridge Texts in Applied Mathematics, pp. 52–101. Cambridge, UK: Cambridge University Press.
40. Harmer GP, Abbott D. 1999 Losing strategies can win by Parrondo's paradox. *Nature* **402**, 864–864. (doi:10.1038/47220)
41. Harmer GP, Abbott D, Taylor PG, Parrondo JM. 2001 Brownian ratchets and Parrondo's games. *Chaos* **11**, 705–714. (doi:10.1063/1.1395623)
42. Jian-Jun S, Qi-Wen W. 2014 Beyond Parrondo's paradox. *Sci. Rep.* **4**, 4244. (doi:10.1038/srep04244)

43. Wen T, Cheong KH, Lai JW, Koh JM, Koonin EV. 2022 Extending the lifespan of multicellular organisms via periodic and stochastic intercellular competition. *Phys. Rev. Lett.* **128**, 218101. (doi:10.1103/PhysRevLett.128.218101)
44. Cheong KH, Koh JM, Jones MC. 2019 Paradoxical survival: examining the Parrondo effect across biology. *BioEssays* **41**, 1900027. (doi:10.1002/bies.201900027)
45. Reed FA. 2007 Two-locus epistasis with sexually antagonistic selection: a genetic Parrondo's paradox. *Genetics* **176**, 1923–1929. (doi:10.1534/genetics.106.069997)
46. Tan ZX, Cheong KH. 2017 Nomadic-colonial life strategies enable paradoxical survival and growth despite habitat destruction. *Elife* **6**, e21673. (doi:10.7554/eLife.21673)
47. Baker DJ *et al.* 2016 Naturally occurring p16 Ink4a-positive cells shorten healthy lifespan. *Nature* **530**, 184–189. (doi:10.1038/nature16932)
48. Beauséjour CM, Krtolica A, Galimi F, Narita M, Lowe SW, Yaswen P, Campisi J. 2003 Reversal of human cellular senescence: roles of the p53 and p16 pathways. *EMBO J.* **22**, 4212–4222. (doi:10.1093/emboj/cdg417)
49. Nichols J, Lima A, Rodríguez TA. 2022 Cell competition and the regulative nature of early mammalian development. *Cell Stem Cell* **29**, 1018–1030. (doi:10.1016/j.stem.2022.06.003)